Competition constrains parasite adaptation to thermal heterogeneity

Samuel TE Greenrod[1#], Daniel Cazares[1], Weronika Slesak[1], Tobias E Hector[1], R. Craig MacLean[1,2], Kayla C King[1,3,4,#]

[1] Department of Biology, University of Oxford, Oxford, UK

[2] All Souls College, High Street, Oxford OX1 4AL, UK

[3] Department of Zoology, University of British Columbia, Vancouver, Canada

[4] Department of Microbiology & Immunology, University of British Columbia, Vancouver, Canada

[#]Correspondence: greenrodsam@gmail.com (Samuel Greenrod); kayla.king@ubc.ca (Kayla King)

Abstract

Temporal thermal heterogeneity is expected to favour intermediate, generalist phenotypes that can maintain growth across a broad thermal range but have sub-optimal growth at any single temperature. Yet, thermal variation typically occurs in the presence of additional selection pressures which may interact to constrain adaptation to temperature. We propagated competing lytic viral parasites (bacteriophages ϕ14-1 and ϕLUZ19) of *Pseudomonas aeruginosa* under fluctuating temperatures (37-42°C) in monoculture and in co-culture. Without competition, fluctuating temperatures favoured intermediate thermal phenotypes in the phage ϕ14-1 and resulted in more variable evolutionary outcomes compared to static conditions. However, co-selection from fluctuating temperatures and competition led to restricted thermal adaptation, slower evolutionary rates, and fewer putative adaptive mutations in the ϕLUZ19 competitor. Our study highlights the potential for reduced adaptive capacity in interacting communities amidst global climate change.

Introduction

Thermal heterogeneity plays a key role in shaping species' evolutionary trajectories. Spanning a broad range of timescales, temperatures fluctuate across multi-year periods (ENSO), between seasons, and even on the order of hours through diurnal (24-hour) cycles. Very slow or rapid thermal fluctuation frequencies, with respect to generation times, typically lead to similar adaptation to static environments through selective sweeps by specialist variants [1,2]. Moderate fluctuation frequencies select for thermal generalists which have intermediate phenotypes across temperatures [1–3]. Generalist phenotypes often arise through the acquisition of multiple specialist mutations [3] or single pleiotropic mutations [4]. Thermal heterogeneity can also promote diversifying selection [5–7] leading to the maintenance of thermal specialist sub-populations [6]. The mechanisms of adaptation to thermal heterogeneity depend on the fluctuation frequency relative to generation time [8]; fluctuations that far exceed generation times in fast-replicating species may favour specialists, but in slow-replicating species may instead select for generalists.

Thermal heterogeneity typically occurs in the context of multiple selective pressures. For example, warming can impose selection on species that are simultaneously adapting to other abiotic stressors or to interactions with predators, competitors, or antagonists [9,10]. The presence of multiple selection pressures can constrain evolution rates through combined negative effects on species fitness which reduce population sizes and mutational supply [11,12]. Co-selection can also restrict adaptation through pleiotropic fitness trade-offs; high fitness under one stressor reduces fitness under another [13,14]. Temporal thermal heterogeneity is expected to promote genetic diversification by increasing niche differences [16] and so may offset the diversity-suppressing impacts of co-selection. However, some studies have indicated that co-selection involving temporal heterogeneity can exacerbate evolutionary constraint [17–19]. The ability of species to adapt to thermal heterogeneity amidst other selection pressures plays an important role in the maintenance of global biodiversity and species extinction risk [11,20–22].

Parasites provide an ideal group of organisms to study adaptation to thermal heterogeneity. Parasites are often exposed to diverse environments and stressors across their multi-stage life cycles. They can have both free-living, vector-based, and host-associated life stages [23]. By moving through numerous external environments during and between replicative cycles, parasites experience high temporal thermal heterogeneity (Greenrod et al., in press; [24]). During the infection stage, parasites can also induce fevers in hosts, driving thermal changes [25]. Finally, parasites are expected to face increasingly frequent thermal extremes as a result of global climate change [26]. While contending with variable thermal environments, parasites must adapt to host immune responses [27] and competition with co-infecting parasites in the same host population or individual [28]. Within and between-host competition are primary determinants of parasite virulence [29] signifying that interactions between competition and environment-based selection can shape parasite evolution [30].

We predicted that thermal heterogeneity would select for generalist parasite populations, which have intermediate phenotypes, and promote genetic diversity [1]. We also predicted that co-selection with other environmental stressors would constrain parasite adaptation [17]. We passaged two lytic viral parasites (thermal generalist ϕLUZ19 and specialist ϕ14-1) under a fluctuating thermal regime (37-42°C) in the absence and presence of a phage competitor. Phages evolved with a static bacterial host, *Pseudomonas aeruginosa*. We compared populations evolved under fluctuating temperatures concurrently with those evolved under a static regime (37°C and 42°C), the latter presented in ref. [31]. We evaluated phage phenotypic adaptation through growth assays at 37°C and 42°C. We also conducted phage population sequencing to identify adaptive mutations and measure evolutionary rates.

Methods and Materials

Strains, Storage, and Culture Conditions

This study builds on a previously published experimental framework [31] using the same bacterial host and bacteriophage strains. *Pseudomonas aeruginosa* PAO1 was used as the non-evolving bacterial host throughout. Two lytic phages, ϕLUZ19 and ϕ14-1, were used due

to their known thermal response differences: ϕLUZ19 performs well at both 37°C and 42°C, while ϕ14-1 is growth-restricted at 42°C [31,32]. Phage lysates and bacterial stocks were prepared as in refs [31,32].

Experimental Evolution

The experimental evolution design closely followed that of ref. [31] with additional treatments incorporating fluctuating temperatures. Phages were serially passaged for 15 days under four conditions: monoculture and co-culture, each at either static or fluctuating temperatures (daily shifts between 37°C and 42°C). Each treatment included six independent replicate populations initiated from a single ancestral lysate.

Phages were propagated without shaking with a non-evolving ancestral PAO1 bacterial host. For the initial passage, ancestral phage lysates were diluted to 10^8 PFU/ml and 300µl were added to 2.7ml 10^8 CFU/ml bacterial culture in loose-lid 14ml falcon tubes. Phage co-culture populations were prepared by combining 150µl each of ϕLUZ19 and ϕ14-1 10^8 PFU/ml lysates prior to mixing with bacteria. The initial passage phage densities were ~10^7 PFU/ml resulting in a phage/bacteria ratio (multiplicity of infection, MOI) = ~0.1. Following addition of bacterial cultures, tubes were incubated statically at 37°C or 42°C in circulating water baths for 8h. Fluctuating passages started and ended at 37°C.

After incubation, phage populations were harvested by centrifugation (3,095×g, 5 min) to pellet bacteria, followed by sterile filtration through 0.2µm filters. Filtrates were stored at 4°C. In subsequent passages, 300µl of lysate was transferred into fresh PAO1 cultures.

Phage Quantification

Phage titres were determined via the double-layer overlay method [33] following the same protocols as in refs [31,32]. Briefly, bacterial lawns were prepared by mixing 10mL of melted LB-top agar with 300µL of a *P. aeruginosa* PAO1 overnight culture. Phage lysates were serially diluted, and 10µL was spotted onto the bacterial lawns. After incubating plates for 6–8 h at 37°C, spots with the highest number of discernible plaques were counted and reported. ϕLUZ19- or ϕ14-1-resistant PAO1 strains were used for selective plating enabling separate counting of ϕLUZ19 and ϕ14-1 densities in co-cultures. These resistant strains were derived by isolating colonies growing on high titre phage plaques and confirmed via sequencing [31]. All monoculture and co-culture samples were quantified using the appropriate resistant strains to ensure consistency.

Phage Separation and Concentration

To generate high-titre and pure phage lysates for downstream assays and sequencing, we employed selective double-layer overlays with resistant hosts. Briefly, phages and ϕLUZ19- or ϕ14-1-resistant PAO1 strains were seeded into top agar plates to allow phage propagation. Phages were extracted from plates by scraping top-agar into 15ml falcon tubes containing 5ml of phage buffer (NaCl (100 mM), $MgSO_4$ (10 mM), $CaCl_2$ (5 mM), Tris-HCl (pH 8) (50 mM), Gelatin (0.01%)). Tubes were mixed overnight after which phages were separated from top agar using sterile-filtration. This process was performed three times to ensure removal of

118 phage competitors from co-culture populations. The purification and extraction protocols
119 were identical to those described in ref. [31].

120 **Phage Growth Rate Assays**

121 The thermal phenotypes of purified evolved phage populations relative to the ancestor was
122 assessed by measuring phage and bacterial growth across an 8h window under static
123 incubation at 37°C and 42°C. Phage lysates were diluted to 10^5 PFU/ml and 300uL was mixed
124 with 2.7ml of 10^8 CFU/ml wild-type PAO1 to a final MOI = ~0.0001. ϕLUZ19 was sampled at
125 2h, 4h, and 8h; ϕ14-1 at 4h and 8h due to delayed replication. Phage quantification was
126 performed through sterile-filtration through 0.22µm filter plates (Agilent) followed by
127 centrifugation at 2,230xg for 5 mins before spotting onto resistant PAO1 double-layer overlay
128 plates. Each growth rate assay included a single replicate of each evolved phage population
129 and three replicates of the phage ancestor. Growth rate assays were repeated three times
130 across a two-week period to produce three technical replicates.

131 **Phage Population Genomics**

132 ***DNA Extraction and Sequencing***

133 Phage DNA was extracted from purified lysates as described in [31]. Briefly, ancestral and
134 evolved phage lysates were treated with DNase and RNase to remove bacterial DNA and RNA.
135 Phage particles were lysed using lysis (AL) buffer and proteinase K. Cell debris was
136 precipitated using precipitation (N4) buffer and removed. Finally, DNA was precipitated and
137 washed using isopropanol and ethanol. DNA quality was assessed with NanoDrop 2000c
138 (Thermo Scientific) and quantified with Qubit 4 (Thermofisher). Short-read Illumina
139 sequencing was performed by AZENTA/GENEWIZ using their Microbe-EZ pipeline for evolved
140 and ancestral populations. Bacterial genomes (wild-type and phage-resistant strains) were
141 sequenced by MicrobesNG using long-read approaches.

142 ***Sequence Analysis***

143 Phage reads were pre-processed with Trim Galore (v.0.5.0)
144 (https://github.com/FelixKrueger/TrimGalore) and downsampled using bbnorm from the
145 bbmap package (v.39.18) (https://sourceforge.net/projects/bbmap/). Reads were then
146 mapped to de novo ancestral assemblies generated with shovill (v1.1.0)
147 (https://github.com/tseemann/shovill) using Bowtie2 (v.2.3.4.2) [34]. Variants were
148 identified using breseq (v.0.36.1) [35]. Ancestral assemblies were annotated with prokka
149 (v.1.14.5) [36], guided by the NCBI GenBank file for each phage (ϕ14-1: NC_011703; ϕLUZ19:
150 NC_010326).

151 Wild-type and resistant PAO1 genomes were assembled using Autocycler (v. 0.4.0) [37] and
152 polished via Polypolish (v. 0.6.0) [38]. Final assemblies were re-oriented with Dnaapler (v.
153 1.2.0) [39] and annotated using prokka (v.1.14.5) [36]. The workflow was deployed using a
154 Dockerised Nextflow pipeline (v. 1.0.2) available
155 at https://doi.org/10.5281/zenodo.15706447. Mutations in resistant PAO1 strains were
156 identified by mapping long reads to the wild-type assembly with minimap2 (v.2.24) [40] and

157 variant calling with medaka (v.2.1) (https://github.com/nanoporetech/medaka). All
158 bioinformatic analyses were conducted with default parameters.

159 **Statistical Analyses and Visualisation**

160 All statistical analyses and data visualisation were conducted using packages in R (v.4.3.2) and
161 RStudio [41,42]. Data wrangling was performed using "Tidyverse" (v.2.0.0) R packages [43].
162 Phage growth and evolution rates were compared between evolution treatments using linear
163 mixed effect models with the "lme4" (v.1.1-36) R package [44] where the response variable
164 was phage density (pfu/ml) or genetic distance from ancestor, the explanatory variables were
165 an interaction term between evolution treatment and temperature, and batch was a random
166 effect. Within-group variation in genetic distance from ancestor was analysed using Levene's
167 test. The prevalence of unique compared to shared mutations across evolution treatments
168 was analysed using Fisher's exact test. Phage genetic distance between groups was also
169 compared by constructing neighbour-joining trees based on Euclidean genetic distance using
170 the "ggtree" (v.3.10.1) R package [45]. Data and code used in analyses can be found at
171 https://github.com/SamuelGreenrod/Evol_fluctuating.

172

173 ## Results

174 **Fluctuating temperatures select for generalist phenotypes in monoculture**

175 Fluctuating environments can favour generalists with intermediate phenotypes across
176 conditions [1]. Given ϕ14-1 has previously been shown to grow poorly at 42°C, we
177 hypothesised that ϕ14-1 populations passaged under fluctuating conditions would rapidly
178 adapt to 42°C but have lower fitness at 37°C and 42°C compared to static evolved populations.
179 In monoculture, ϕ14-1 densities increased during 37°C passages but decreased in 42°C
180 passages (Fig. 1A). As phage lysates were diluted 10-fold in between passages, phage density
181 decreases reflect lower than 10-fold ϕ14-1 population growth during 42°C passages. ϕLUZ19
182 monoculture populations reached and then maintained high densities in all passages. This
183 phage showed low variation in inter-passage densities.

184 We assessed phage evolution by measuring the growth rates of static and fluctuating evolved
185 populations relative to the ancestral phage through growth assays at 37°C and 42°C (Fig. 1B).
186 We found that growth rates of both phages in monoculture depended on the interaction
187 between evolution treatment and assay temperature (ϕ14-1: $F_{3,29} = 125.8$, $p < 0.001$; ϕLUZ19:
188 $F_{3,29} = 96.0$, $p < 0.001$). At 42°C, ϕ14-1 fluctuating populations were found to have an
189 intermediate phenotype between those evolved under static conditions. ϕ14-1 fluctuating
190 populations had significantly higher growth rates at 42°C than 37°C static populations ($t(29)$
191 $= -12.4$, $p < 0.001$) but lower growth rates than 42°C static populations ($t(29) = 12.7$, $p < 0.001$).
192 At 37°C, ϕ14-1 fluctuating populations had no significant difference to static populations
193 possibly due to phage growth being measured after phages had reached carrying capacity
194 (see ref. [31]). For ϕLUZ19, fluctuating evolved populations had significantly higher growth at
195 42°C than 37°C static populations ($t(29) = -19.3$, $p < 0.001$). However, growth was not

196 significantly different to 42°C evolved populations (t(29) =-1.65, p = 0.37). The opposite
197 findings were observed at 37°C; fluctuating evolved populations had significantly higher
198 growth rates than those evolved at 42°C but similar growth rates to 37°C evolved populations
199 (42°C static: t(29) = -5.2, p < 0.001; 37°C static: t(29) = -0.99, p = 0.75).

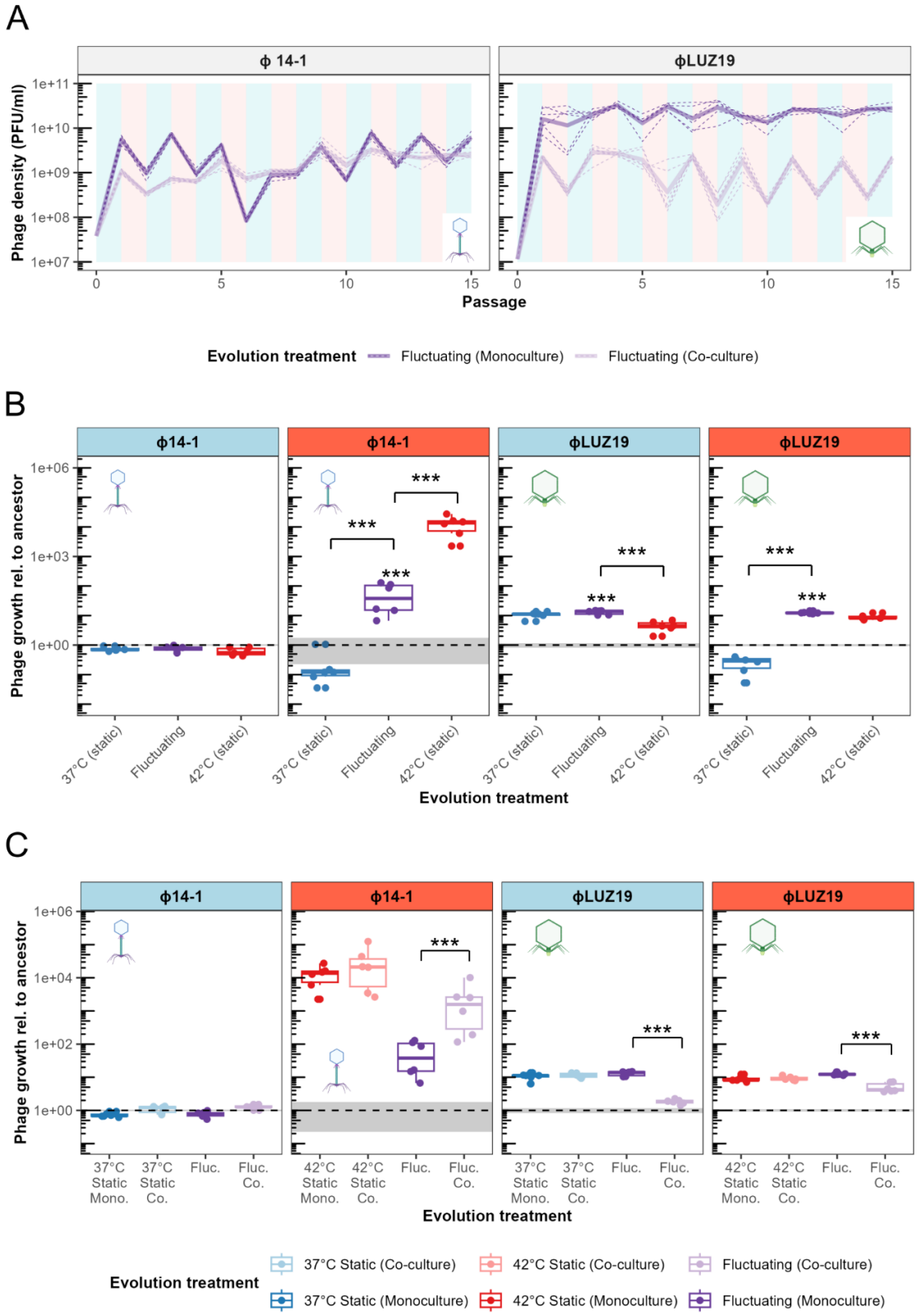

Figure 1. Co-selection in communities constrains adaptation to thermal fluctuations. A) Population dynamics of phages passaged in monoculture and co-culture under fluctuating temperatures. Values show densities at the end of each passage prior to dilution. As phage lysates were diluted 10-fold in between passages, density decreases reflect less than 10-fold population growth during passages. Plot background colour reflects the temperature during that passage where light blue is 37°C and light red is 42°C. Phage icons illustrate the two different phages used in the experiments (ϕ14-1, myovirus in blue; ϕLUZ19, autographivirus in green) [46] and are used hereafter to refer to phages in figures. **B**) Fluctuating and static temperature evolved population growth rates relative to the ancestor. Growth rates were measured after 2h for ϕLUZ19 and 4h for ϕ14-1. Six biological replicates were assayed, and data points show the average of three technical replicates. Panel strip colour reflects the temperature that growth was tested at where light blue is 37°C and light red is 42°C. Fluctuating populations are presented in purple with 37°C static populations in blue and 42°C static populations in red. Ancestral growth is shown by dashed grey line with standard errors shown as a grey box (n = 3). *** = $p < 0.001$. Absence of asterisk reflects non-significance. Static monoculture temperature data was adapted from ref. [31]. **C**) Growth rates of fluctuating and static temperature monoculture evolved populations compared to co-culture evolved populations. Boxes are coloured by evolution treatment with monoculture in dark (37°C static in blue, 42°C static in red, and fluctuating in purple) and co-culture in light (37°C static in light blue, 42°C static in light red, and fluctuating in light purple). Assay temperature and significance values are presented as in Fig. 1B. Six biological replicates were assayed and data points show the average of three technical replicates. Ancestral growth rates and significance signs are presented as in Fig. 1B. Static co-culture data was adapted from ref. [31].

Co-selection from fluctuating temperatures and competition constrains thermal adaptation

The presence of additional selection pressures is expected to constrain adaptation to fluctuating temperatures by reducing mutational supply and compounding fitness trade-offs [11,18,19]. We hypothesised that phages evolved under co-selection from fluctuating temperatures and competition would have lower growth rates at 37°C and 42°C than those evolved under static temperatures or fluctuating monoculture conditions. While ϕ14-1 densities fluctuated between passages in monoculture, co-culture densities rapidly increased and then stabilised between passages (Fig. 1A). In contrast, ϕLUZ19 populations were stable in monoculture, but during fluctuations in co-culture, experienced high growth at 37°C and low growth at 42°C.

We then assessed evolved phage growth rates at 37°C and 42°C (Fig. 1C). We found a significant interaction between evolution treatment (monoculture and co-culture) and temperature regarding growth rates for both phages (ϕ14-1: $F_{6,59} = 75.0$, $p < 0.0001$; ϕLUZ19: $F_{6,59} = 103.5$, $p < 0.0001$). While competition had no impact on the growth rates of static ϕ14-1 populations (37°C: $t(59) = -0.78$, $p = 0.99$; 42°C: $t(59) = -0.98$, $p = 0.99$), fluctuating co-culture evolved populations had significantly higher growth rates at 42°C compared to populations evolved in monoculture ($t(59) = -6.7$, $p < 0.0001$). No significant difference was observed at 37°C ($t(59) = -1.0$, $p = 0.99$). Similar to ϕ14-1, there was no impact of competition on static evolved ϕLUZ19 population growth rates (37°C: $t(59) = -0.42$, $p = 1.0$; 42°C: $t(59) = -0.21$, $p = 1.0$). However, ϕLUZ19 populations evolved with fluctuations and competition had

242 significantly lower growth rates at both 37°C and 42°C compared to monoculture (37°C: $t(59)$
243 $= 10.1$, $p < 0.0001$; 42°C: $t(59) = 4.9$, $p < 0.001$).

244

245 **Fluctuating environments favour specialist mutations**

246 Fluctuating temperatures generally select for multiple specialist mutations [3]. We
247 hypothesised that fluctuating evolved populations would show genetic similarities to both
248 high and low temperature static populations. Phage genomic evolution was assessed by
249 constructing neighbour-joining trees of end-point populations based on Euclidean genetic
250 distances (Fig. 2A). Genetic distances were calculated based on the presence and frequency
251 of genetic variants (SNPs, indels) that had > 10% frequency. Fluctuating evolved populations
252 did not form a unique clade but instead were found to co-locate with either high or low
253 temperature static populations. ϕ14-1 fluctuating populations were distributed across the
254 tree and generally did not cluster with static populations. Conversely, ϕLUZ19 fluctuating
255 populations were primarily found within the 42°C static clade.

256 We further analysed static and fluctuating population genetic similarities by measuring
257 evolution rates based on Euclidean genetic distance from ancestor (Fig. 2B). For ϕ14-1,
258 fluctuating evolved populations had significantly lower evolution rates than 42°C static
259 populations ($t(15) = -4.1$, $p < 0.01$). However, evolution rates were equal between fluctuating
260 and 37°C static populations ($t(15) = -0.51$, $p = 0.87$). There was no significant difference in
261 evolution rates between ϕLUZ19 fluctuating populations and either 37°C or 42°C static
262 populations (37°C: $t(15) = -0.46$, $p = 0.89$; 42°C: $t(15) = -0.75$, $p = 0.74$). Notably, ϕ14-1
263 fluctuating populations had significantly greater within-group variation in evolution rates
264 compared to 42°C static populations ($t(15) = 2.9$, $p < 0.05$) but not 37°C static populations
265 ($t(15) = -0.70$, $p = 0.77$). ϕLUZ19 fluctuating populations had no significant difference in
266 within-group variation compared to static populations (37°C: $t(15) = 2.0$, $p = 0.15$; 42°C: $t(15)$
267 $= -0.10$, $p = 0.99$).

268 We then determined the prevalence of individual genetic variants (SNPs, indels) that were
269 unique to or shared between evolution treatments (Fig. 2C). Only putative adaptive variants
270 with >20% frequency were included. For ϕ14-1, 2/11 (18%) of 37°C static variants and 5/15
271 (33%) of 42°C static variants were shared with other evolution treatments compared to 4/9
272 (44%) variants in fluctuating evolved populations. For ϕLUZ19, shared variants constituted
273 8/32 (35%) of 37°C static and 9/20 (45%) of 42°C static variants compared to 12/17 (71%) in
274 fluctuating evolved populations. To assess the overall impact of evolution treatment on the
275 ratio of unique and shared mutations, we pooled mutations from ϕ14-1 and ϕLUZ19
276 observing a significant difference in the prevalence of shared mutations relative to unique
277 mutations between evolution treatments (Fisher's exact test: $p < 0.05$). Significant differences
278 were not observed when analysing phages independently (ϕ14-1, $p = 0.47$; ϕLUZ19, $p = 0.08$).
279 ϕ14-1 fluctuating mutations were primarily shared with 42°C static populations (Fig. S1). In
280 contrast, ϕLUZ19 fluctuating mutations were shared equally with 37°C and 42°C static
281 populations.

282 Finally, we investigated which mutations drove clustering between fluctuating and static
283 populations (Fig. S2; Table S1). While ϕ14-1 fluctuating and 37°C static populations showed
284 little clustering, two fluctuating populations clustered with the 42°C static clade. These two
285 replicate populations contained parallel deletions in a hypothetical protein with high
286 similarity to a DNA ligase (BlastP: 97.47% identity, 95% sequence overlap with Pseudomonas
287 phage PhL_UNISO_PA-DSM_ph0031 DNA ligase protein), previously identified in all ϕ14-1
288 42°C static populations [31]. The clustering of 5/6 ϕLUZ19 fluctuating populations with the
289 42°C static populations were attributed to parallel insertions in an intergenic region between
290 two hypothetical proteins. This intergenic insertion was also previously identified in all
291 ϕLUZ19 42°C static populations [31].

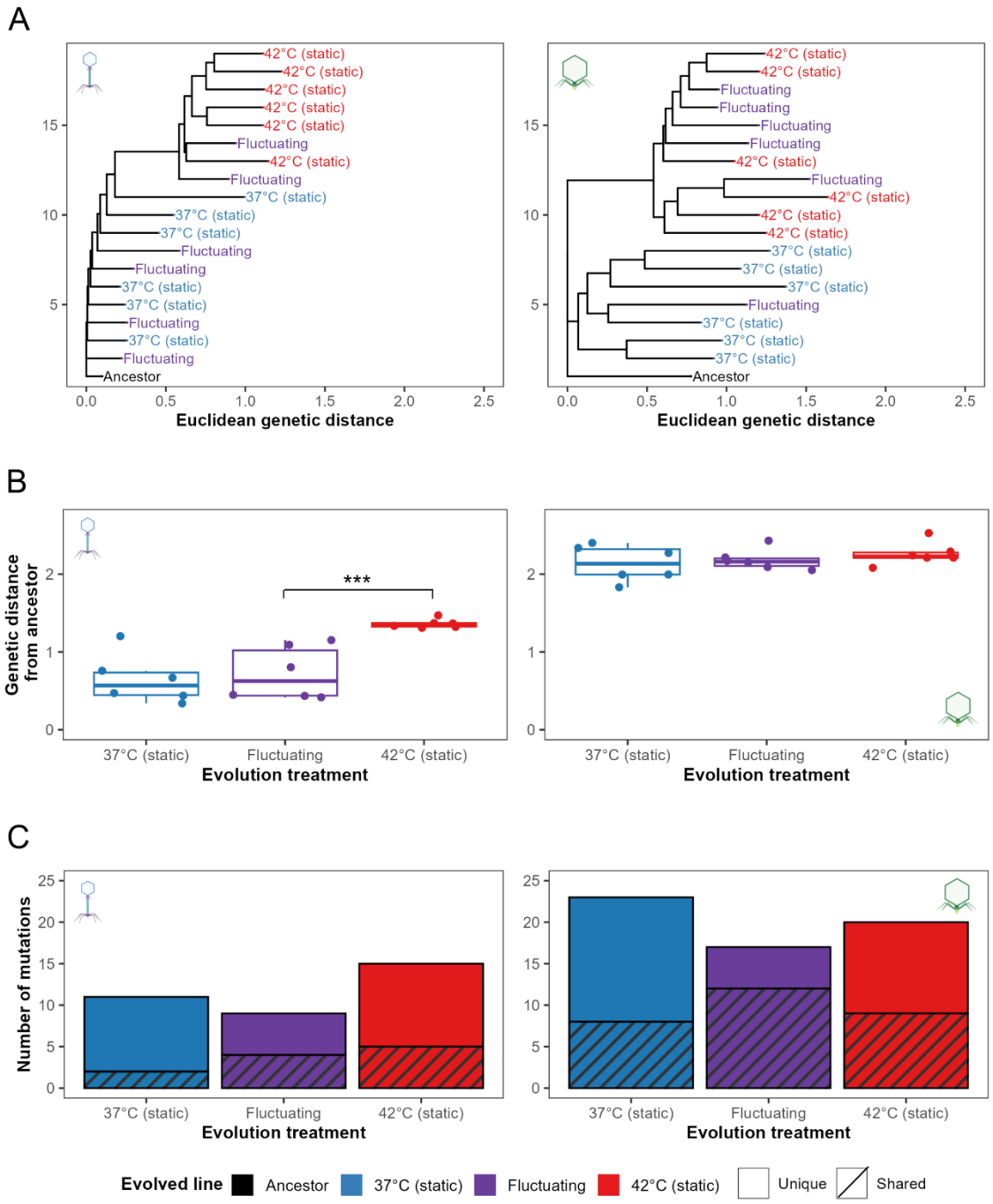

292 **Figure 2. Fluctuating temperatures select for specialist mutations. A**) Neighbour-joining
293 trees of evolved and ancestral phage populations constructed using Euclidean genetic
294 distances. Genetic distances were calculated based on the presence and frequency of
295 mutations present at > 10% frequency. Tree is rooted at the ancestor and populations are
296 coloured by evolved treatment. **B**) Phage evolution rates, measured based on Euclidean
297 genetic distance from the ancestor, for evolved monoculture phage populations. *** = $p <$
298 0.001. **C**) Stacked bar charts show the number of high frequency (>20% frequency), putative
299 adaptive variants that are unique to or shared between evolution treatments. Bars are
300 coloured by evolution treatment. Unique genes are shown as clear bars and shared genes are
301 shown as striped bars. Static temperature data was adapted from ref. [31].

302

303 **Co-selection constrains molecular evolution**

304 By reducing growth rates, co-selection from fluctuating temperatures and competition are
305 expected to reduce evolution rates and restrict the acquisition of adaptive mutations [11].
306 Due to their elevated growth rates, we hypothesised that ϕ14-1 fluctuating co-culture
307 populations would have higher evolution rates than monoculture populations. No significant
308 difference in evolution rate was observed for ϕ14-1 co-culture populations compared to
309 monoculture populations ($F_{1,10} = 4.1$, $p = 0.07$) (Fig. 3A). However, non-significance was driven
310 by a single low evolution rate replicate in the co-culture treatment; when the replicate was
311 removed, co-culture populations had significantly greater evolution rates than monoculture
312 ($F_{1,9} = 8.6$, $p < 0.05$). We also found no significant difference in within-group variation in
313 evolution rates between monoculture and co-culture populations ($t(10) = 1.50$, $p = 0.17$),
314 although the difference was also significant once the low evolution rate co-culture replicate
315 was removed ($t(10) = 3.6$, $p < 0.01$).

316 For ϕLUZ19, we hypothesised that fluctuating co-culture populations would have lower
317 evolution rates than monoculture populations due to the suppression of ϕLUZ19 by ϕ14-1.
318 ϕLUZ19 fluctuating co-culture populations had significantly lower evolution rates than
319 monoculture populations ($F_{1,10} = 470$, $p < 0.001$). We further hypothesised that ϕLUZ19
320 fluctuating co-culture populations, but not ϕ14-1 populations, would have lower evolution
321 rates than 37°C or 42°C static co-culture populations. Evolution rates were equal between co-
322 culture populations for ϕ14-1 ($F_{2,15} = 1.2$, $p = 0.3$) (Fig. 3B). However, ϕLUZ19 fluctuating co-
323 culture populations were found to have significantly lower evolution rates than both 37°C
324 static and 42°C static monoculture populations (37°C: $t(15) = 4.5$, $p < 0.01$; 42°C: $t(30) = 3.0$, p
325 < 0.05).

326 Finally, we assessed the impact of competition on the acquisition of high frequency mutations
327 (> 20% frequency) in fluctuating populations (Fig. S3). For ϕ14-1, while populations no longer
328 acquired singleton mutations, all populations acquired a deletion or SNP in a putative DNA
329 ligase gene. Mutations in this gene are thought to contribute to high temperature adaptation
330 [31] and were also found in the two monoculture populations which clustered with 42°C static
331 populations in Fig. 2A. For ϕLUZ19, while co-culture populations maintained mutations in tail

332 fiber genes, the populations no longer acquired singleton mutations or the intergenic
333 insertion associated with 42°C static populations.

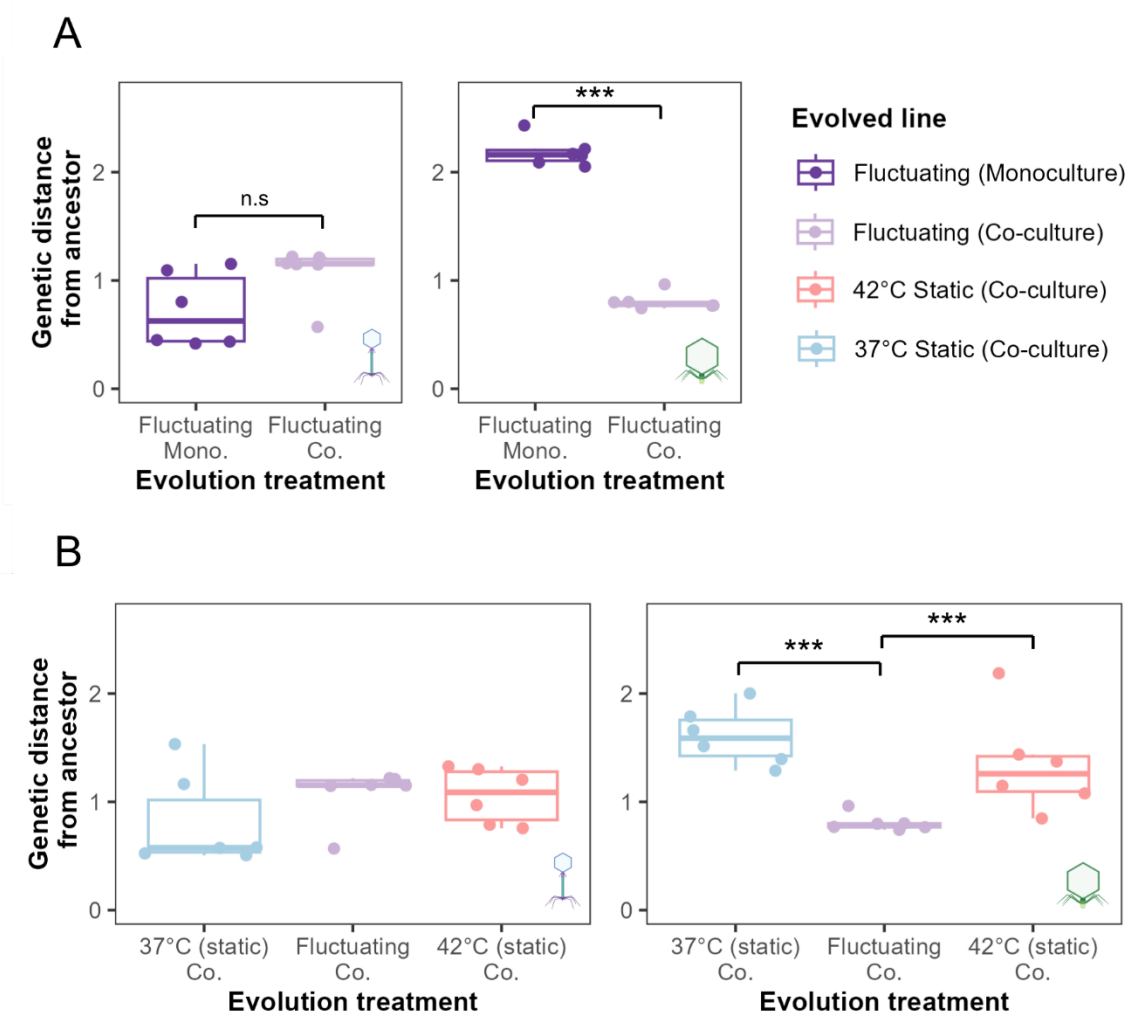

334

335 **Figure 3. High environmental complexity constrains evolution rates**. **A**) Evolution rates,
336 measured based on Euclidean genetic distance from the ancestor, of phage populations
337 evolved under fluctuating temperatures in monoculture (deep purple) and co-culture (light
338 purple). **B**) Evolution rates of 37°C static, fluctuating, and 42°C static co-culture populations.
339 Plot layout is the same as panel A. *** = $p < 0.001$. N.S is used to denote lack of statistical
340 significance. Static temperature data was adapted from ref. [31].

341

342 ## Discussion

343 Under fluctuating selection, both phages were found to rapidly evolve increased growth rates
344 at high temperatures. For phage ϕ14-1, fluctuating temperatures favoured intermediate
345 thermal phenotypes with lower growth rates at high temperatures compared to phages
346 evolved under static temperatures. The evolution of intermediate growth rates is likely due
347 to weaker selection for adaptation to high temperatures in the fluctuating treatment.

Alternatively, adaptation to high temperatures may be constrained during fluctuations due to fitness trade-offs at lower temperatures [47]. For phage ϕLUZ19, fluctuating temperature populations had the same growth rates as static-evolved populations when measured at their evolved temperature. Given ϕLUZ19 was shown to exhibit growth rate trade-offs under static selection [31], this finding is indicative of a no-cost generalist strategy [48]. The lack of growth rate costs may reflect an epistatic pleiotropy, whereby the costs of adaptive mutations depend on the genetic background [48]. Costs may also occur in unmeasured traits such as virulence [49] or tolerance to other stresses [14]. These findings highlight that, while fluctuating temperatures select for greater high temperature growth, the exact phenotypic outcomes of fluctuating selection vary between phage taxa.

We found that fluctuating temperatures resulted in more variable evolutionary trajectories; while static evolved populations generally formed clusters, fluctuating populations were genetically similar to both 37°C and 42°C static evolved populations. Further, we found that parallel mutations acquired under fluctuating selection were the same as those previously identified in static evolved populations [31]. These findings could be explained by historical contingency [50] whereby random mutations that are adaptive at low or high temperatures become fixed in a subset of populations [6]. Depending on the timing of mutation appearance, fluctuating populations may then resemble individual static environments. Fluctuating environments have also been shown to select for mutations conferring fitness in the most extreme environment [51]. The clustering of ϕLUZ19 fluctuating populations with 42°C static populations likely reflects selective sweeps combined with asymmetrical selection where 42°C adaptive variants are fixed more rapidly.

While fluctuating environments can promote genetic diversification, co-selection with other environmental stressors can constrain adaptation [11]. Uiterwaal et al [18] showed that combined fluctuating temperatures and predation restricted adaptation to both selection pressures in *Paramecium caudatum* populations. Similar findings have also been observed in *Daphnia magna* with co-selection from thermal fluctuations and predation/pollutants [19,52]. We found that combined fluctuating temperature- and competition-based selection constrained both thermal adaptation and slowed evolutionary rates in phage ϕLUZ19. Further, co-selection resulted in greater ϕLUZ19 evolutionary constraint with fluctuating temperatures than static temperatures. The negative effects of combined environmental stressors are often non-additive and instead exhibit synergies [11]. We have previously shown that selection from high temperatures synergises with competition to constrain ϕLUZ19 evolution rates [31]. The present study extends these findings by showing that the selective synergy between temperature and competition is greater under fluctuating temperatures than static temperatures. One potential explanation for these findings is that fluctuating environments reduce the strength of selection for adaptive mutations [53]. Weaker directional selection combined with suppression by competitors may constrain both the supply and fixation of beneficial mutations leading to particularly low evolution rates.

Anthropogenic activities, including global climate change, mean that species are facing increasingly variable and complex environments [54]. With ongoing global biodiversity loss, species must adapt to tolerate environmental stressors to avoid extinctions. Our findings

highlight that while species can rapidly adapt in response to thermal variation, co-selection with other stressors, such as competition, may restrict species adaptive capacity. These results have particular relevance for parasites which must simultaneously adapt to both thermal heterogeneity, community competition in coinfections, and host immune responses. With global parasite biodiversity at risk due to climate change [26], evolutionary constraint caused by co-selection may prevent parasite adaptation to thermal stress and further increase the probability of parasite extinctions. Future studies should consider the evolution-constraining effects of co-selection when assessing species extinction risk in thermally variable environments.

Acknowledgments

We thank R. Salguero-Gomez, T. Richards, T. Barraclough, and K. Foster for feedback on the experimental design and results. This work was supported by the Biotechnology and Biosciences Research Council (BB/T008784/1) to S.T.E.G. as well as the Natural Environment Research Council (NE/X000540/1) and NSERC Canada Excellence Research Chair to K.C.K. The funders had no role in study design, data collection and interpretation, or the decision to submit the work for publication. Phage sequence reads are accessible on NCBI (https://www.ncbi.nlm.nih.gov/) under BioProject ID: PRJNA1334331.

References

1. Kassen R. The experimental evolution of specialists, generalists, and the maintenance of diversity. Journal of Evolutionary Biology. 2002;15(2):173–90.

2. Sachdeva V, Husain K, Sheng J, Wang S, Murugan A. Tuning environmental timescales to evolve and maintain generalists. Proceedings of the National Academy of Sciences. 2020 Jun 9;117(23):12693–9.

3. Kassen R, Bell G. Experimental evolution in Chlamydomonas. IV. Selection in environments that vary through time at different scales. Heredity. 1998;80(6):732–41.

4. Lambros M, Pechuan-Jorge X, Biro D, Ye K, Bergman A. Emerging Adaptive Strategies Under Temperature Fluctuations in a Laboratory Evolution Experiment of Escherichia Coli. Front Microbiol. 2021 Oct 22;12:724982.

5. Sandberg TE, Lloyd CJ, Palsson BO, Feist AM. Laboratory Evolution to Alternating Substrate Environments Yields Distinct Phenotypic and Genetic Adaptive Strategies. Appl Environ Microbiol. 2017 Jun 16;83(13):e00410-17.

6. Abdul-Rahman F, Tranchina D, Gresham D. Fluctuating Environments Maintain Genetic Diversity through Neutral Fitness Effects and Balancing Selection. Molecular Biology and Evolution. 2021 Oct 1;38(10):4362–75.

7. Harrison E, Laine AL, Hietala M, Brockhurst MA. Rapidly fluctuating environments constrain coevolutionary arms races by impeding selective sweeps. Proc Biol Sci. 2013 Aug 7;280(1764):20130937.

8. Chesson P. Mechanisms of Maintenance of Species Diversity. Annual Review of Ecology, Evolution, and Systematics. 2000 Nov 1;31(Volume 31, 2000):343–66.

9. Gilchrist GW. Specialists and Generalists in Changing Environments. I. Fitness Landscapes of Thermal Sensitivity. The American Naturalist. 1995;146(2):252–70.

10. Gunderson AR, Armstrong EJ, Stillman JH. Multiple Stressors in a Changing World: The Need for an Improved Perspective on Physiological Responses to the Dynamic Marine Environment. Annual Review of Marine Science. 2016 Jan 3;8(Volume 8, 2016):357–78.

11. Hector TE, Hoang KL, Li J, King KC. Symbiosis and host responses to heating. Trends in Ecology & Evolution. 2022 Jul 1;37(7):611–24.

12. Crain CM, Kroeker K, Halpern BS. Interactive and cumulative effects of multiple human stressors in marine systems. Ecology Letters. 2008;11(12):1304–15.

13. Hiltunen T, Cairns J, Frickel J, Jalasvuori M, Laakso J, Kaitala V, et al. Dual-stressor selection alters eco-evolutionary dynamics in experimental communities. Nat Ecol Evol. 2018 Dec;2(12):1974–81.

14. Burmeister AR, Fortier A, Roush C, Lessing AJ, Bender RG, Barahman R, et al. Pleiotropy complicates a trade-off between phage resistance and antibiotic resistance. Proceedings of the National Academy of Sciences. 2020 May 26;117(21):11207–16.

15. Schou MF, Engelbrecht A, Brand Z, Svensson EI, Cloete S, Cornwallis CK. Evolutionary trade-offs between heat and cold tolerance limit responses to fluctuating climates. Science Advances. 2022 May 27;8(21):eabn9580.

16. van Houte S, Padfield D, Gómez P, Luján AM, Brockhurst MA, Paterson S, et al. Compost spatial heterogeneity promotes evolutionary diversification of a bacterium. J Evol Biol. 2021 Feb;34(2):246–55.

17. Yamamichi M, Letten AD, Schreiber SJ. Eco-evolutionary maintenance of diversity in fluctuating environments. Ecol Lett. 2023 Sep;26 Suppl 1:S152–67.

18. Cairns J, Borse F, Mononen T, Hiltunen T, Mustonen V. Strong selective environments determine evolutionary outcome in time-dependent fitness seascapes. Evol Lett. 2022 Jun 1;6(3):266–79.

19. Uiterwaal SF, Lagerstrom IT, Luhring TM, Salsbery ME, DeLong JP. Trade-offs between morphology and thermal niches mediate adaptation in response to competing selective pressures. Ecology and Evolution. 2020;10(3):1368–77.

20. Barbosa M, Pestana J, Soares AMVM. Predation Life History Responses to Increased Temperature Variability. PLoS One. 2014 Sep 24;9(9):e107971.

21. D. Vinebrooke R, L. Cottingham K, Norberg J Marten Scheffer, I. Dodson S, C. Maberly S, Sommer U. Impacts of multiple stressors on biodiversity and ecosystem functioning: the role of species co-tolerance. Oikos. 2004;104(3):451–7.

465 22. Halpern BS, Walbridge S, Selkoe KA, Kappel CV, Micheli F, D'Agrosa C, et al. A Global Map of
466 Human Impact on Marine Ecosystems. Science. 2008 Feb 15;319(5865):948–52.

467 23. Bellard C, Bertelsmeier C, Leadley P, Thuiller W, Courchamp F. Impacts of climate change on
468 the future of biodiversity. Ecology Letters. 2012;15(4):365–77.

469 24. Nguyen PL, Gokhale CS. On multiple infections by parasites with complex life cycles. Oikos.
470 2025;2025(4):e10493.

471 25. Silva LM, King KC, Koella JC. Dissecting transmission to understand parasite evolution. PLoS
472 Pathog. 2025 Mar 25;21(3):e1012964.

473 26. Oakley MS, Gerald N, McCutchan TF, Aravind L, Kumar S. Clinical and molecular aspects of
474 malaria fever. Trends in Parasitology. 2011 Oct 1;27(10):442–9.

475 27. Carlson CJ, Burgio KR, Dougherty ER, Phillips AJ, Bueno VM, Clements CF, et al. Parasite
476 biodiversity faces extinction and redistribution in a changing climate. Science Advances. 2017
477 Sep 6;3(9):e1602422.

478 28. Buckingham LJ, Ashby B. Coevolutionary theory of hosts and parasites. j evol Biol. 2022 Feb
479 1;35(2):205–24.

480 29. Pedersen AB, Fenton A. Emphasizing the ecology in parasite community ecology. Trends in
481 Ecology & Evolution. 2007 Mar 1;22(3):133–9.

482 30. Hasik AZ, King KC, Hawlena H. Interspecific host competition and parasite virulence evolution.
483 Biology Letters. 2023 May 3;19(5):20220553.

484 31. Limberger R, Fussmann GF. Adaptation and competition in deteriorating environments.
485 Proceedings of the Royal Society B: Biological Sciences. 2021 Mar 10;288(1946):20202967.

486 32. Greenrod ST, Cazares D, Slesak WA, Hector T, MacLean RC, King KC. Evolutionary rescue
487 accelerates competitive exclusion in a parasite community [Internet]. bioRxiv; 2025 [cited 2025
488 Sep 28]. p. 2025.09.25.678511. Available from:
489 https://www.biorxiv.org/content/10.1101/2025.09.25.678511v1

490 33. Greenrod STE, Cazares D, Johnson S, Hector TE, Stevens EJ, MacLean RC, et al. Warming alters
491 life-history traits and competition in a phage community. Applied and Environmental
492 Microbiology. 2024 Apr 16;0(0):e00286-24.

493 34. Kropinski AM, Mazzocco A, Waddell TE, Lingohr E, Johnson RP. Enumeration of Bacteriophages
494 by Double Agar Overlay Plaque Assay. In: Clokie MRJ, Kropinski AM, editors. Bacteriophages:
495 Methods and Protocols, Volume 1: Isolation, Characterization, and Interactions [Internet].
496 Totowa, NJ: Humana Press; 2009 [cited 2023 Jun 2]. p. 69–76. (Methods in Molecular
497 Biology™). Available from: https://doi.org/10.1007/978-1-60327-164-6_7

498 35. Langmead B, Salzberg SL. Fast gapped-read alignment with Bowtie 2. Nat Methods. 2012
499 Apr;9(4):357–9.

500 36. Deatherage DE, Barrick JE. Identification of mutations in laboratory evolved microbes from
501 next-generation sequencing data using breseq. Methods Mol Biol. 2014;1151:165–88.

502 37. Seemann T. Prokka: rapid prokaryotic genome annotation. Bioinformatics. 2014 Jul
503 15;30(14):2068–9.

504 38. Wick RR, Howden BP, Stinear TP. Autocycler: long-read consensus assembly for bacterial
505 genomes [Internet]. bioRxiv; 2025 [cited 2025 Jul 29]. p. 2025.05.12.653612. Available from:
506 https://www.biorxiv.org/content/10.1101/2025.05.12.653612v1

507 39. Wick RR, Holt KE. Polypolish: Short-read polishing of long-read bacterial genome assemblies.
508 PLOS Computational Biology. 2022 Jan 24;18(1):e1009802.

509 40. Bouras G, Grigson SR, Papudeshi B, Mallawaarachchi V, Roach MJ. Dnaapler: A tool to reorient
510 circular microbial genomes. Journal of Open Source Software. 2024 Jan 11;9(93):5968.

511 41. Li H. Minimap2: pairwise alignment for nucleotide sequences. Bioinformatics. 2018 Sep
512 15;34(18):3094–100.

513 42. RStudio Team. RStudio: Integrated Development for R. [Internet]. RStudio, PBC, Boston, M;
514 2020. Available from: http://www.rstudio.com/

515 43. R Core Team. R: A language and environment for statistical computing. [Internet]. Foundation
516 for Statistical Computing, Vienna, Austria.; 2021. Available from: https://www.R-project.org/

517 44. Wickham H, Averick M, Bryan J, Chang W, McGowan LD, François R, et al. Welcome to the
518 Tidyverse. Journal of Open Source Software. 2019 Nov 21;4(43):1686.

519 45. Bates D, Mächler M, Bolker B, Walker S. Fitting Linear Mixed-Effects Models Using lme4.
520 Journal of Statistical Software. 2015 Oct 7;67:1–48.

521 46. Yu G, Smith DK, Zhu H, Guan Y, Lam TTY. ggtree: an r package for visualization and annotation
522 of phylogenetic trees with their covariates and other associated data. Methods in Ecology and
523 Evolution. 2017;8(1):28–36.

524 47. Tabare E, Glonti T, Cochez C, Ngassam C, Pirnay JP, Amighi K, et al. A Design of Experiment
525 Approach to Optimize Spray-Dried Powders Containing Pseudomonas aeruginosaPodoviridae
526 and Myoviridae Bacteriophages. Viruses. 2021 Oct;13(10):1926.

527 48. Visher E, Boots M. The problem of mediocre generalists: population genetics and eco-
528 evolutionary perspectives on host breadth evolution in pathogens. Proc Biol Sci. 2020 Aug
529 26;287(1933):20201230.

530 49. Remold S. Understanding specialism when the jack of all trades can be the master of all.
531 Proceedings of the Royal Society B: Biological Sciences. 2012 Oct 24;279(1749):4861–9.

532 50. Ashrafi R, Bruneaux M, Sundberg LR, Pulkkinen K, Valkonen J, Ketola T. Broad thermal
533 tolerance is negatively correlated with virulence in an opportunistic bacterial pathogen.
534 Evolutionary Applications. 2018;11(9):1700–14.

535 51. Blount ZD, Lenski RE, Losos JB. Contingency and determinism in evolution: Replaying life's tape.
536 Science. 2018 Nov 9;362(6415):eaam5979.

537 52. Arribas M, Kubota K, Cabanillas L, Lázaro E. Adaptation to Fluctuating Temperatures in an RNA
538 Virus Is Driven by the Most Stringent Selective Pressure. PLOS ONE. 2014 Jun 25;9(6):e100940.

53. Barbosa M, Inocentes N, Soares AMVM, Oliveira M. Synergy effects of fluoxetine and variability in temperature lead to proportionally greater fitness costs in Daphnia: A multigenerational test. Aquatic Toxicology. 2017 Dec 1;193:268–75.

54. Cvijović I, Good BH, Jerison ER, Desai MM. Fate of a mutation in a fluctuating environment. Proc Natl Acad Sci U S A. 2015 Sep 8;112(36):E5021–8.

55. Jaureguiberry P, Titeux N, Wiemers M, Bowler DE, Coscieme L, Golden AS, et al. The direct drivers of recent global anthropogenic biodiversity loss. Science Advances. 2022 Nov 9;8(45):eabm9982.

572 ## Extended data

573

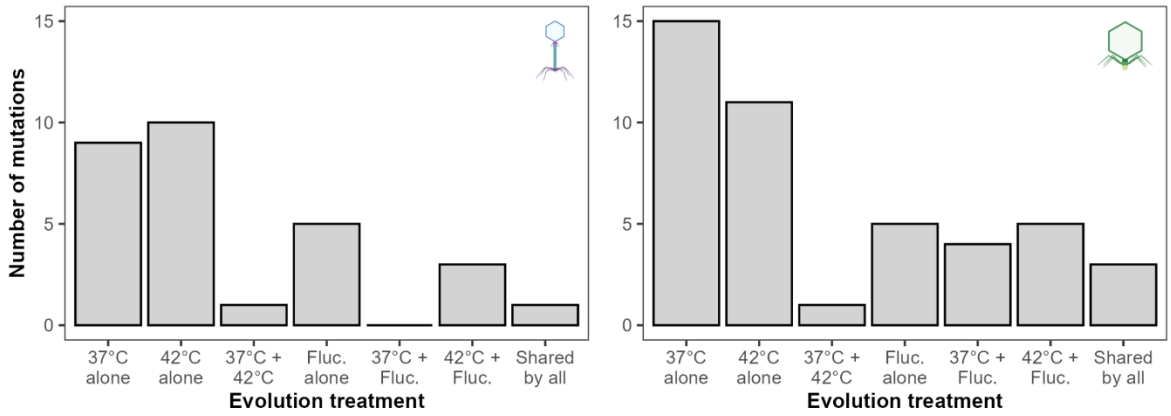

574

575 **Figure S1. Bar charts show the number of high frequency variants (> 20% frequency) that are unique**
576 **to or shared between evolution treatments.** Variants are shown as either unique to individual
577 evolution treatments, shared between two treatments, or shared by all three. Static temperature data
578 was adapted from ref. [31].

579

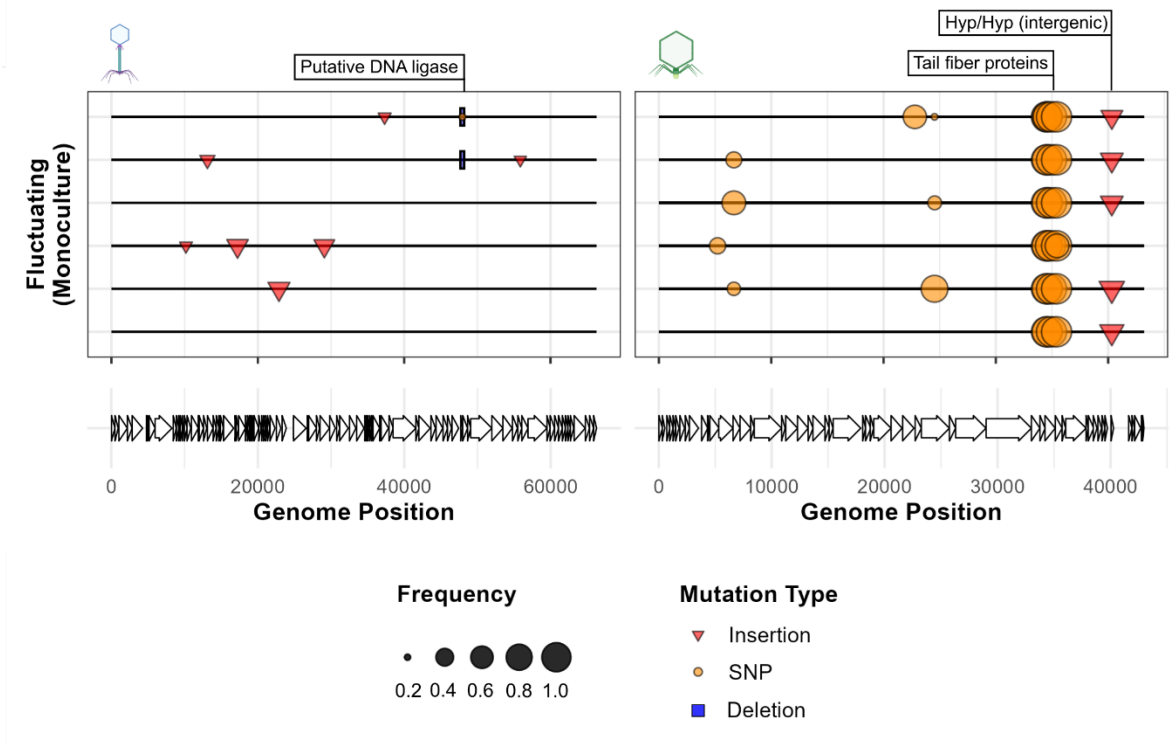

580

581 **Figure S2. Fluctuating temperatures select for specialist mutations.** Mutation plots show genetic
582 variants associated with fluctuating temperatures in monoculture in phage populations. Lines
583 represent individual biological replicates. Symbols within plots show variants across the phage
584 genome at > 20% prevalence and which were not observed in the ancestral population. Length of
585 deletion bars represent the size of deletion except for the ϕ14-1 deletion at ~48kb which is a 1bp

586 deletion but given a fixed size for visibility. Labels show gene annotations for mutations found in 37°C
587 and 42°C evolved populations [31]. Putative DNA ligase in ϕ14-1 was originally annotated a
588 hypothetical protein but has high homology to Pseudomonas phage PhL_UNISO_PA-DSM_ph0031
589 DNA ligase protein.

590

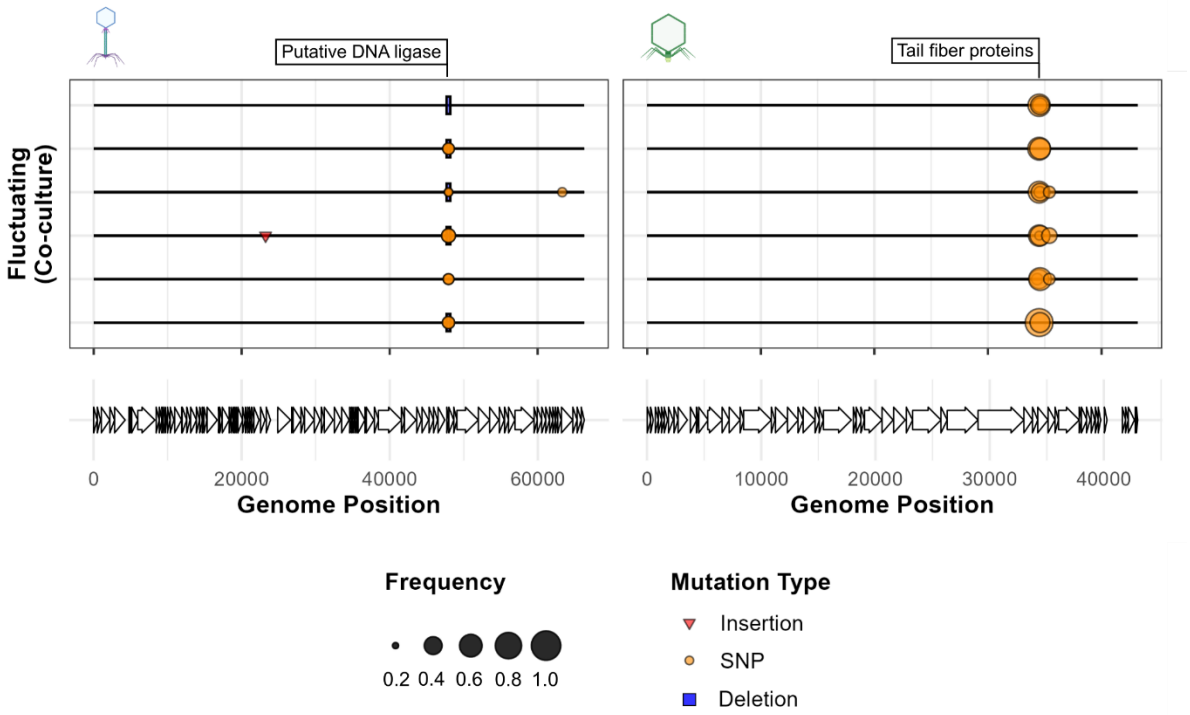

591

592 **Figure S3. Competition restricts the acquisition of high frequency mutations.** Mutation plots show
593 genetic variants associated with fluctuating temperatures in co-culture in phage populations. Lines
594 represent individual biological replicates. Symbols within plots show variants across the phage
595 genome at > 20% prevalence and which were not observed in the ancestral population. Length of
596 deletion bars represent the size of deletion except for the ϕ14-1 deletion at ~48kb which is a 1bp
597 deletion but given a fixed size for visibility. Labels show gene annotations for mutations found in 37°C
598 and 42°C evolved populations [31]. Putative DNA ligase in ϕ14-1 was originally annotated a
599 hypothetical protein but has high homology to Pseudomonas phage PhL_UNISO_PA-DSM_ph0031
600 DNA ligase protein.

601